



Published in final edited form as:

Mol Pharm. 2010 December 6; 7(6): 2280–2288. doi:10.1021/mp100242r.

Disruption of the mucus barrier by topically applied exogenous particles

Shayna L. McGill* and Hugh D. C. Smyth

Division of Pharmaceutics, University of Texas at Austin, College of Pharmacy, 1 University Station A1920, Austin, TX, 78712 U.S.A

Abstract

The mucus barrier is well established as a formidable barrier to exogenous substances and forms the first line of defense for mucosal surfaces. Drugs and particle systems are known to be significantly hindered via a variety of interactions with mucus and some efforts have been reported that can mitigate these interactions. We investigated topically applied particulate systems (nano and micro) for their potential to interact with mucus and influence on the diffusion of model drugs across the mucus barrier. Functionalized polystyrene nanoparticles and microparticles and diesel particulate matter were topically applied to established in vitro mucus models. Particle treated mucus was then assessed, compared to controls, for drug permeation rates. The average permeation rate of drugs increased 2-fold following the application of particles to mucus compared to permeation of the same drug through mucus alone. In some cases permeation enhancement of small model drugs was over 5 times that of controls. Assessment of particle physicochemical properties also indicated that significant interactions occurred between mucus and the particles as determined by zeta potential changes and size changes. Collectively this work supports the hypothesis that topically applied particles interact with the mucus barrier causing disruption of this barrier allowing for increased drug permeation. These findings have implications for improved drug delivery and enhanced environmental exposure to exogenous substances.

Keywords

Mucus; particles; drug delivery; diffusion

Introduction

Physical barriers such as skin and mucus membranes are the first line of defense for the innate immune system¹. Mucosal epithelial surfaces such as the nasopharynx, lungs, reproductive tissues, and gastrointestinal organs are protected by a layer of mucus that can trap exogenous substances until they can be removed by clearance mechanisms such as ciliary movement¹. To successfully perform this role of protection mucus maintains a complex molecular composition and structure². The main component that is responsible for its viscous and elastic gel-like properties is the glycoprotein mucin². These mucins are large molecules (0.5 – 20 MDa) that are highly glycosylated. These oligosaccharide chains (5–15 monomers) are attached to a protein core to form a so called “bottle brush” configuration^{2,3}. The chemical composition results in electrostatic, hydrophobic, and H-bonding interactions. It is therefore not surprising that many different interactions can occur between exogenous

*To whom correspondence should be addressed: Shayna L. McGill, BSci, Division of Pharmaceutics, University of Texas at Austin, College of Pharmacy, 1 University Station A1920, Austin, TX 78712-0126, U.S.A., smcgill@mail.utexas.edu.

substances and mucus that are adhesive and significantly influence diffusion of solutes through this complex network structure^{2,3}.

The importance of the mucus barrier in health and disease is well documented^{2,4-7}. Several studies have shown that the transport of certain drugs may be significantly inhibited through mucus⁸⁻¹⁰. In the gastrointestinal tract, it is well established that the mucus layer is the first line of defense against secreted acid and pepsin⁶. This stable unstirred layer forms a diffusion barrier to pepsin, preventing proteolysis of the underlying epithelial cells. In peptic ulcer disease the rate of peptic degradation of the mucus barrier is increased. Moreover, other damaging agents such as ethanol and aspirin can rapidly permeate the mucus barrier, and may induce ulcers by damaging the underlying epithelium. Similarly, in the respiratory epithelium, the presence of mucus has been shown to significantly limit the effectiveness of viral gene therapy vectors¹¹⁻¹³. In another example of the functional properties of the mucus barrier several groups have studied the entrapment and transport of nanoparticles in cervical mucus and cystic fibrosis mucus samples¹⁴⁻¹⁷.

Despite this recognition of the formidable barrier and importance of the mucus lining on epithelial surfaces for drug delivery and solute diffusion, relatively few studies have investigated what external factors may influence its integrity^{18,19}.

In the studies reported in this paper, for the first time to our knowledge, we demonstrate that topically applied particles can significantly disrupt the mucus barrier. We demonstrate this disruption phenomenon in established models of mucus using nanoparticles, microparticles, and diesel particulate matter and is diagramed in figure 1. The effects of these particles on mucus were assessed using two model drug species. In addition, we provide evidence of how the particles may interact with mucus to induce such changes in the rate of diffusion of low molecular weight drugs.

Materials and Methods

Materials

Sigma mucin from porcine stomach type 2 and type 3 were used for the models of mucus (Type 2 M2378-100G, batch 019K1222, Sigma Aldrich, St. Louis, MO, USA; Type 3 M1778-10G, batch 098K7025, Sigma Aldrich, St. Louis, MO, USA). Four particle types were purchased from Invitrogen: FluoSpheres carboxylate- and amine-modified microspheres 1 micron yellow-green fluorescent (F8823, Lot 543029, Invitrogen, Eugene, OR, USA; F8765, Lot 434725, Invitrogen, Eugene, OR, USA); FluoSpheres carboxylate- and amine-modified microsphere 0.2 um (200 nm) red fluorescent (F8810, Lot 459418, Invitrogen, Eugene, OR, USA; F8763, Lot 531683, Invitrogen, Eugene, OR, USA). Diesel particulate matter was supplied by Jacob McDonald, PhD (Lovelace Respiratory Research Institute, Albuquerque, NM, USA). Fluorescein sodium salt (fluorescein; F6377, batch 064K0153, Sigma Aldrich, St. Louis, MO, USA) and rhodamine B (R6626, batch 063K3406, Sigma Aldrich, St. Louis, MO, USA) were used as model drugs.

Mucus models

The mucus models used in these studies have been widely employed in other permeability studies^{8,15}. A 20% w/v concentration of type 3 (unpurified) was mixed with double distilled water in a shaking incubator overnight. A cystic fibrosis sputum model was made according to Dawson et al using the type 2 (partially purified) mucin at 60 mg/mL mixed with 3.2 mg/mL lecithin, and 32 mg/mL BSA in buffer containing 05mM Na⁺, 75 mM Cl⁻, 20 mM Hepes, pH 7.4, for 48 hours¹⁵.

Rheological Characterization of Mucus Models

Dynamic oscillatory measurements were performed at controlled deformation using a TA Instruments AR-G2 Rheometer (TA Instruments, DE, USA). Storage, loss, and complex moduli were measured as a function of both deformation and frequency. Linear viscoelastic region was determined with deformation sweep under: deformation interval from 0.08–10 at a frequency of 10Hz; frequency sweeps were performed over two frequency intervals (0.1–50Hz and 0.5–15Hz) at constant deformation (0.5).

Physical Characterization of Particles

Nanoparticle hydrodynamic diameters were characterized using a ZetaPlus Zeta Potential Analyzer with a Multi Angle Particle Sizing Option installed (Brookhaven Instruments Corporation, Holtsville, NY) operating with a 25 mW laser at a wavelength of 635 nm. Detection of scattered light was at 90° to the incident beam. Each sample was subjected to three two-minute measurements. Typically, solutions of up to 2×10^{-4} mg/mL in 1 mM KCl were used for the characterizations, at a temperature of 25°C.

ζ-Potential measurements were conducted using electrophoretic light scattering, also using the Brookhaven ZetaPlus, on the same samples that were sized. Scattered light was detected at 15° (175° to the incident beam) at a temperature of 25°C. Each sample was subjected to 10 measurements, with a 5 sec delay between each measurement.

A Supra 40VP (Carl Zeiss SMT AG, Germany) scanning electron microscope (SEM) was used to determine the morphology of the synthesized particles. Samples were prepared for imaging by drop drying onto an aluminum stage. To prevent charging of the samples, they were sputter coated with platinum/palladium using a Cressington 208 benchtop sputter coater (Watford, UK).

Specific surface area of diesel particulate matter was obtained using the BET method on a Quantachrome Monosorb (Quantachrome Instruments, Florida, USA). Diesel particulates were degassed at 80 °C for 12 hours under nitrogen gas flow of 20 psi. Following degassing particulates were analyzed. Specific surface area of monodisperse spheres were determined using calculation of their surface area based on their well defined size and known densities.

Permeability Experiments

Permeability of fluorescein or rhodamine B was determined by using a modified diffusion cell setup. The diffusion cell setup consisted of Snapwells inserts, that act as the donor side, placed atop 24 well tissue culture plates containing 3 mL of PBS buffer as the acceptor side (Corning Snapwells™, CLS3802, Corning, USA; Multiwell Primaria™ 24 well, Falcon™, Becton Dickinson Labware Franklin Lakes, NJ, USA). Mucus models were plated onto the Snapwells™ at a volume of 250 μL. Particles were applied topically followed by the topical application of the model drugs fluorescein or rhodamine B. Samples were removed from the acceptor side at predetermined time points and analyzed using a plate reader set up for fluorescence intensity measurements at excitations and emissions of 460 nm and 515 nm for fluorescein and 514 nm and 630 nm for rhodamine B (Infinite M200, Tecan Group LTD, Switzerland).

Permeability rates (cm/sec) were calculated using an Excel spreadsheet (Microsoft Office 2008, version 12.25, Microsoft Corp.). For statistical evaluation of the data, analysis of variance (one-way) and post-hoc comparisons (Tukey method) were performed using StatPlus (StatPlus:Mac2009, AnalystSoft).

Results

Representative examples of the rheological properties of the two *in vitro* mucin models, unpurified reconstituted and CF sputum buffered mucin, are given in Fig. 2a and 2b. Elastic (G') and viscous (G'') moduli of the two mucus models are presented as functions of oscillatory frequencies.

Particles were characterized using SEM (Fig. 3a, 3b). The uniform monodisperse size (200 nm and 1 micron) and shape (spherical) as claimed by manufacturers specification were confirmed for polystyrene beads. Due to the uniformity of the beads, the specific surface area was calculated using the known density of polystyrene. The surface area for the 200 nm particles was 28.6 m²/g and 5.7 m²/g for the 1 micron particles. Diesel particulate matter (DPM) was also characterized using SEM (Fig. 3c) and dynamic light scattering (mean diameter 287 nm). The specific surface area for the DPM was determined to be 45.0±0.5 m²/g as determined by B.E.T. measurements.

Drug permeability studies were performed using the unpurified mucin model using either fluorescein or rhodamine B as model drugs under various experimental conditions. When the polystyrene particles (carboxyl functionalization) were topically added to the mucus model, fluorescein permeability rates were increased 2.4 fold for 200 nm particles and 1.6 fold for 1 micron particles compared to untreated controls (Fig. 4a). Rhodamine B exhibited permeability increases of 4.9 fold and 1.6 fold when particles of 200 nm and 1 micron, respectively, were added (Fig. 4b), though overall rhodamine B permeability was generally less than that of fluorescein.

The influence of different surface functionalization of the particles on drug permeability was also assessed. Particles functionalized with either amine or carboxyl groups were used and topically applied to the mucus model prior to drug permeation studies. The surface charges of these particles range between 0.1 and 2 mEq/g and therefore they remain stable in relatively high concentrations of electrolytes²⁰. Permeation rate of fluorescein increased through mucus model when treated with either amine or carboxyl particles (Fig. 5a). For the study performed using rhodamine B as the model drug, overall permeation increases of the drug compared to controls were observed but no significant differences in rates from the different particle types were observed (Fig. 5b).

To assess the mucus barrier disruption more generally, an additional mucus model was selected for comparison. This model, named cystic fibrosis like mucus (or CF mucus) is also derived from literature reports in which researchers have sought to mimic mucus in CF by preparing the *in vitro* mucus that has similar composition to that of CF patients' sputum samples¹⁵. In Figure 6a and 6b, a comparison of the permeability enhancement ratios for mucus models, drugs, particle sizes, and particle types is presented. Mucus barrier disruption as measured by the permeation enhancement ratio of the hydrophilic model drug, fluorescein was no different when comparing the two mucus models. However, significant differences in rhodamine B permeation enhancement ratio were detected due to the differences in the mucus model composition.

The permeation enhancement of each drug as a result of mucus barrier disruption by the different particle sizes is shown in Figure 7. For 1 micron particle treatments, either amine or carboxyl functionalized, no differences were observed between fluorescein or rhodamine b permeation enhancement. Smaller 200 nm particles appear to have a more significant effect (statistical differences detected for both rhodamine and fluorescein) but the magnitude of enhancement was greater for rhodamine B.

To probe particle-mucin interactions on the molecular scale, DLS particle size measurements and Zeta potential were performed on particles before and after association with mucus (Fig. 8). Particles were either treated with mucin or control (buffer) and then the particles were washed extensively by repeated centrifugation. Strongly bound mucin molecules on the particle surfaces could therefore be detected using both size and charge measurements performed on the washed particles. Both amine and carboxyl particles treated in mucin had significant increases in particle size compared to particles that were only treated in buffer (Fig. 8a). The zeta potentials were also found to significantly change (to similar magnitudes) for both particle types after mucin treatment (Fig. 8b).

To extend our investigations further, mucus models were then topically treated with diesel particulate matter (instead of monodisperse polystyrene particles) and permeation of drug was determined as described previously (Fig. 9). Consistent with the findings above, statistically significant increases in permeation rates of fluorescein and rhodamine were observed following exposure of mucus to topically applied nanoparticles. The only combination that did not result in permeation increases due to particle treatment was for rhodamine B in the CF-like mucus model (also consistent with observations above).

Discussion

To the best of our knowledge these studies are the first to demonstrate that exogenous particles topically applied to mucus can disrupt the mucus barrier. This disruption was significant, often yielding greater than 2 fold increases in permeation of fluorescein (mw = 376) and rhodamine B (mw = 479) through different models of mucus.

Mucus Barrier Properties

Reconstituted mucus derived from pig gastric, human cervical, and tracheobronchial mucins have similar mucus structures, and have been found to have physiological relevant compositions and rheological properties^{8,9,15}. As such several studies have used these models to investigate drug and nanoparticle permeability through these barriers^{8,15,19}. The microstructure of mucus is condensed and represents a highly viscoelastic network that impedes transport of drugs^{8,9}, macromolecules^{10,17}, nanoparticles^{14,16}, gene delivery systems^{12,13}, and viruses^{11,17}. In some of these studies, the particle interaction with mucus has been explored in more detail¹⁵⁻¹⁷. In these reports, nanoparticles intended as drug and/or gene delivery carriers were entrapped by mucin interactions limiting their transport and inhibiting drug/gene delivery to the target site. These observations are clearly consistent with the intended protective function of mucus, which forms the first and primary barrier on mucosal surfaces.

Using a different approach, we have shown here that particles themselves can interact with mucus and can result in the disruption of the mucus barrier. This particle mediated disruption of mucus leads to apparent pathways so that exogenous substances can pass through the barrier at much faster rates.

Mucus and Particle Characterization

Mucus rheology—Rheological properties of the mucus models were characterized by using the frequency-dependent elastic (G') and viscous (G'') moduli. Our studies show that both unpurified and cystic fibrosis model mucus have increased viscous modulus at higher frequencies, though the unpurified model had relatively high viscous modulus under all frequencies. Our ranges of G' and G'' fit within other models of animal mucus, specifically canine respiratory mucus ($G'=4.7-63$ Pa $G''=1.0-20$ Pa for subglottis; $G'=2.0-80$ Pa $G''=0.5-40$ Pa for tracheal)²². Canine mucus has been used as a model for human respiratory

mucus since the dog lung is similar to the human lung in anatomy and size. Additionally, the tracheal mucus of canine showed similar rigidity to human mucus compared to other animal models (ferret, rabbit, and rat). The mucus models used here were derived from porcine gastric mucins and generally seemed to have consistent ranges of elastic and viscous moduli with those mentioned for pigs ($G' = 0.18\text{--}160$ Pa and $G'' = 0.05\text{--}16$ Pa) primarily for the cystic fibrosis model. It should be mentioned that lower shear rates were used since reconstituted mucus tends to deform at lower shear rates than natural mucus²³. Finally, the bulk G' determined in our studies is in the same range as those determined in human mucus rheological studies¹⁸. In summary, the models selected for use in our studies provide viscoelastic properties that match well with literature findings for the physiological mucus.

Diffusion barrier properties—In addition to rheological characterization of the mucus models, we selected the model drug fluorescein due to its prior use in other studies as a marker of the barrier properties of mucus. Indeed, in these studies fluorescein exhibited permeability through mucus model barriers similar to other literature results^{8,9}. Our experimental set up has small differences in mucus layer thickness, mucus composition, and source compared to other systems described in the literature and therefore small differences in permeability values were expected.

Particle characteristics—To verify that the particle manufacturer's size and shape specifications were accurate for the different particle systems obtained, scanning electron microscopy (SEM) and dynamic light scattering (DLS) were used. Both methods showed that the particles were close to the size ranges that were described in the product information documentation (200 nm and 1 micron), though DLS revealed that the particles were slightly larger. The values of the zeta potential of the particles were also in the range claimed by the manufacturer: -58.74 ± 1.66 mV for carboxyl and -46.03 ± 0.96 mV for amine particles.

Diesel particulate matter generated from combustion can vary according to the methods used to generate and collect it. Therefore characterization was performed to more clearly define the particle properties. SEM images indicated that the particulate matter were highly aggregated clusters of nanoparticles of various shapes and sizes. When BET surface area was determined the specific surface area was an average of 45.0 ± 0.5 m²/g (n=3). This relatively high specific surface area was expected for these fine particulates given their appearance under the SEM.

Disruption of mucus barrier induced by topically applied particles

Influence of particle size—For the particles chosen for this study two different sizes were used (200 nm and 1 μm) to assess the potential role of size in mucus disruption. Overall, both particle sizes indicated increased transport compared to controls. However, the addition of nanoparticles to the mucus membrane was greater in magnitude and statistically significant. The nanometer sized particles present a larger surface area for mucin polymer strand contact and this increased binding areas could result in more extensive interactions. These increased interactions may be responsible for the higher permeation rates of drug through the mucus models presented in our data. Our working hypothesis is that the mesh network of mucus is disrupted by the entrapment of particles because the mucin strands collapse onto the particle surface, opening adjacent pores in the mesh. We imagine this interaction to be similar to that seen when an object becomes stuck in a sticky spider's web and, over time, more and more web strands irreversibly bind to the object's surface, causing larger holes to appear in the overall structure of the web.

Influence of surface chemistry—Particle surface labeling of either amine or carboxyl groups were used to determine any influences these surface groups may have on mucus

disruption. Though slight differences in drug permeation were seen between the two surface groups, none were statistically significant indicating that there was little effect of amine or carboxyl groups on mucus disruption. From our data it can be determined that negatively charged particles, despite the different functional groups used, have the ability to modify the mucus barrier to allow for increased permeation of the model drugs. Dawson et al and Olmsted et al previously found that the same polystyrene particles used in our study exhibited significantly hindered transport rates within mucus^{15,17}.

Influence of the model drug properties—The different model drugs had significantly different permeation rates through the unpurified mucin model, more so than through the CF-like mucin model. The model drugs used were fluorescein sodium salt, a hydrophilic water soluble fluorescent probe, and rhodamine B, a highly lipophilic and water soluble. Rhodamine B transport was the most enhanced when the unpurified mucus barrier was pre-treated with 200 nm nanoparticles of either functionality. However, in the more surfactant rich CF like mucus model (containing lecithin and BSA), rhodamine B permeation was not significantly enhanced by particle pretreatment. On the other hand, fluorescein sodium salt showed an increase in permeation rates compared to controls for both the unpurified and CF-like mucin models. Collectively these observations indicate that drug properties can: (1) significantly change permeability rates through mucus, (2) have significantly different permeation enhancement following mucus barrier disruption, and (3) this behavior is dependent on the composition of the mucus barrier itself. This points to the nature of the drug diffusion and partitioning interactions with the molecular structure of the mucin molecules. We speculate that the more lipophilic drug encountered significantly more hindered transport in mucus with higher mucin content due to partitioning into the lipophilic domains of the mucin. In the case of CF like mucus, a model mucus based on compositional analysis of CF sputum samples, contains high amounts of surface active molecules such as lecithin and BSA. Here the permeability enhancement difference for a lipophilic drug was lost, perhaps due to the less defined hydrophilic-lipophilic molecular structure of the barrier in the presence of surfactants. The hydrophilic drug demonstrated significant permeation enhancement following particulate disruption of the mucus regardless of the mucus model.

Possible Molecular Mechanisms of Disruption

In these studies we also investigated possible evidence for direct interactions between the particles and the mucus. Size and charge characteristics of the particles were determined both before and after interaction with mucus using dynamic light scattering (DLS) and zeta potential, similar to the method used by Dawson and colleagues¹⁵. Particles that had been incubated in mucus (and then extensively washed) showed a statistically significant increase in their particle size. Furthermore, following mucus incubation carboxylate particles and aminated particles appeared to be coated with mucin such that any differences in zeta potentials were eliminated (−36.94 mV and −39.03 mV respectively). Prior to incubation these particle types had significantly different initial zeta potentials (−58.74 mV for carboxyl particles and −46.03 mV for amine particles). These results suggest that particles adsorb mucin to their surfaces with strong interactions resistant to centrifugal separation and washing procedures.

Considering these changes in particle properties following exposure to mucus with the patterns of permeation enhancement described above, we speculate that mucus disruption due to topical application of exogenous particles results from direct disturbance of the mesh network of the mucus barrier. Specifically, we imagine the creation of larger holes and diffusional pathways via collapse of mucin strands onto the high surface area of nanoparticles. This scheme is depicted in Figure 1.

The observation of mucin fibers collapsing onto particles was demonstrated by Olmstead and group¹⁷. They found that herpes simplex virus (HSV) particles would adhere to cervical mucin fibers causing the fibers to collapse around the HSV particles into dense cable-like structures. Larger porous regions formed around the cable-like structures of the mucin. According to Dawson and co-workers particles that were formulated with cationic PLGA and dimethyldioctadecylammonium bromide (DDAB) were able to be transported faster through mucus compared to COOH-polystyrene particles, despite aggregation of the particles within the mucus¹⁵. They speculated that the surface chemistries of the two particle types could affect the transport rates. The slightly larger PLGA-DDAB nanoparticles with higher hydrophilicity may predispose them to greater transport within hydrophilic mucus pores. It was also mentioned that the PLGA-DDAB/DNA nanoparticles may result in the collapse of the mucin fiber strands onto the particle surface and thus causing larger pores. This is consistent with our findings where these induced pores would promote increased transport through mucus.

We observed that the surface chemistry of the particles used in this study had little effect on the transport rates of either fluorescein or rhodamine B through mucus. As demonstrated by zeta potential and particle size measurements, it appears that mucin interactions with the particles, despite different surface functionalization, resulted in coating of the particles with mucins that eliminates differences in particle charge (while inducing increases in particle size). Dawson and coworkers also observed the adsorption of mucin fibers to the surfaces of different particle types that resulted in elimination of the differences in surface chemistry¹⁵. Therefore, mucin appears indiscriminate in its interactions with particles of different surfaces and, can entrap exogenous particles regardless of composition differences that would be necessary to protect from the potentially diverse environmental exposures organisms may be subject to. It must also be noted that Hanes and coworkers have described approaches to overcome these interactions using polyethylene glycol of specific molecular weights and coating densities¹⁶.

The impact of these findings extends beyond drug delivery systems. For example, environmental particulate matter has significant fractions of material in the size and surface area range discussed in this paper. In our initial investigations we selected diesel particulate matter. This nanoparticle system also caused a similar mucus barrier disruption effect indicating that environmental pollutants may also cause mucus modification. This particle induced barrier disruption via inhaled environmental particles has, to the best of our knowledge, not been reported in the scientific literature but has significant implications for allowing increased exposure to other inhaled substances (microbes, carcinogens, etc). Studies investigating these effects are currently underway in our laboratory.

Conclusions

Based on these data, our working hypothesis is that topically applied particles, such as inhaled pollutants, environmental aerosols, and drug delivery systems, may compromise the mucus barrier via strong association of the biopolymers with the surfaces of the particles leading to the opening of new diffusion pathways through the barrier. With this in mind, the potential effects of this compromised barrier may be important in infectious disease, nanotoxicology, and drug delivery and warrant further investigation.

Acknowledgments

The authors would like to acknowledge Stephen Marek for providing the SEM images that were used in this publication. In addition, the assistance of Therapeutex, Drug Dynamics Institute, University of Texas in obtaining the rheological properties of the mucus models is acknowledged. Further acknowledgements go to Jacob McDonald from the Lovelace Respiratory Research Institute for supplying the diesel particulate matter used.

REFERENCES

1. Smith, BT. Concepts in Immunology and Immunotherapeutics. 4th ed.. Smith, BT., editor. American Society of Health-System Pharmacists; 2007.
2. Bansil R, Turner B. Mucin structure, aggregation, physiological functions and biomedical applications. *Current Opinion in Colloid & Interface Science*. 2006; 11(2–3):164–170.
3. Huang, Y.; Peppas, NA. Nanoscale Analysis of Mucus-Carrier Interactions for Improved Drug Absorption. In: Peppas, NA.; Hilt, JZ.; Thomas, JB., editors. *Nanotechnology in Therapeutics: Current Technology and Applications*. UK: Horizon Bioscience; 2007. p. 109-127.
4. Thornton DJ, Sheehan JK. From Mucins to Mucus: Toward a More Coherent Understanding of this Essential Barrier. *The Proceedings of the American Thoracic Society*. 2004; 1:54–61.
5. Girod S, Zahm JM, Plotkowski C, Beck G, Puchelle E. Role of the Physicochemical Properties of Mucus in the Protection of the Respiratory Epithelium. *Eur Respir. J*. 1992; 5:477–487. [PubMed: 1563506]
6. Allen A, Hutton DA, Leonard AJ, Pearson JP, Sellers LA. The Role of Mucus in the Protection of the Gastrointestinal Mucosa. *Scandinavian Journal of Gastroenterology*. 1986; 21:71–78.
7. Slomiany BL, Slomiany A. Role of Mucus in Gastric Mucosal Protection. *J. Physiol Pharmacol*. 1991; 42:147–161. [PubMed: 1782415]
8. Bhat P, Flanagan D, Donovan M. Drug binding to gastric mucus glycoproteins. *International Journal of Pharmaceutics*. 1996; 134(1–2):15–25.
9. Khanvilkar K, Donovan M, Flanagan D. Drug transfer through mucus. *Advanced Drug Delivery Reviews*. 2001; 48(2–3):173–193. [PubMed: 11369081]
10. Saltzman W, Radomsky M, Whaley K, Cone R. Antibody diffusion in human cervical mucus. *Biophysical journal*. 1994; 66(2):508–515. [PubMed: 8161703]
11. Stonebraker JR, Wagner D, Lefensty RW, Burns K, Gendler SJ, Bergelson JM, Boucher RC, O’Neal WK, Pickles RJ. Glycocalyx restricts adenoviral vector access to apical receptors expressed on respiratory epithelium in vitro and in vivo: role for tethered mucins as barriers to luminal infection. *J. of Virology*. 2004; 78:13755–13768. [PubMed: 15564484]
12. Ferrari S, Geddes D, Alton E. Barriers to and New Approaches for Gene Therapy and Gene Delivery in Cystic Fibrosis. *Advanced Drug Delivery Reviews*. 2002; 54:1373–1393. [PubMed: 12458150]
13. Laube B. The expanding role of aerosols in systemic drug delivery, gene therapy, and vaccination. *Respiratory Care*. 2005; 50(9):1161. [PubMed: 16122400]
14. Sanders N, DE SMEDT S, Van Rompaey E, Simoens P, De Baets F, Demeester J. Cystic Fibrosis sputum. A barrier to the transport of nanospheres. *American journal of respiratory and critical care medicine*. 2000; 162:1905–1911. [PubMed: 11069833]
15. Dawson M, Krauland E, Wirtz D, Hanes J. Transport of polymeric nanoparticle gene carriers in gastric mucus. *Biotechnology progress*. 2004; 20(3):851–857. [PubMed: 15176891]
16. Lai S, O’Hanlon D, Harrold S, Man S, Wang Y, Cone R, Hanes J. Rapid transport of large polymeric nanoparticles in fresh undiluted human mucus. *Proceedings of the National Academy of Sciences*. 2007; 104(5):1482.
17. Olmsted S, Padgett J, Yudin A, Whaley K, Moench T, Cone R. Diffusion of macromolecules and virus-like particles in human cervical mucus. *Biophysical journal*. 2001; 81(4):1930–1937. [PubMed: 11566767]
18. Lai S, Wang Y, Cone R, Wirtz D, Hanes J. Altering mucus rheology to “solidify” human mucus at the nanoscale. *PLoS One*. 2009; 4(1):1–6.
19. Bhaskar K, Gong D, Bansil R, Pajevic S, Hamilton J, Turner B, LaMont J. Profound increase in viscosity and aggregation of pig gastric mucin at low pH. *American Journal of Physiology-Gastrointestinal and Liver Physiology*. 1991; 261(5):827.
20. *Molecular Probes: Invitrogen detection technologies. Product Information*. 2004. Working with FluoSpheres® Fluorescent Microspheres: Properties and Modifications; p. 1-5.
21. Lai SK, Wang Y-Y, Wirtz D, Hanes J. Micro- and macrorheology of mucus. *Advanced Drug Delivery Reviews*. 2009; 61(2):86–100. [PubMed: 19166889]

22. Quraishi M, Jones N, Mason J. The rheology of nasal mucus: a review. *Clinical Otolaryngology & Allied Sciences*. 1998; 23(5):403–413. [PubMed: 9800075]

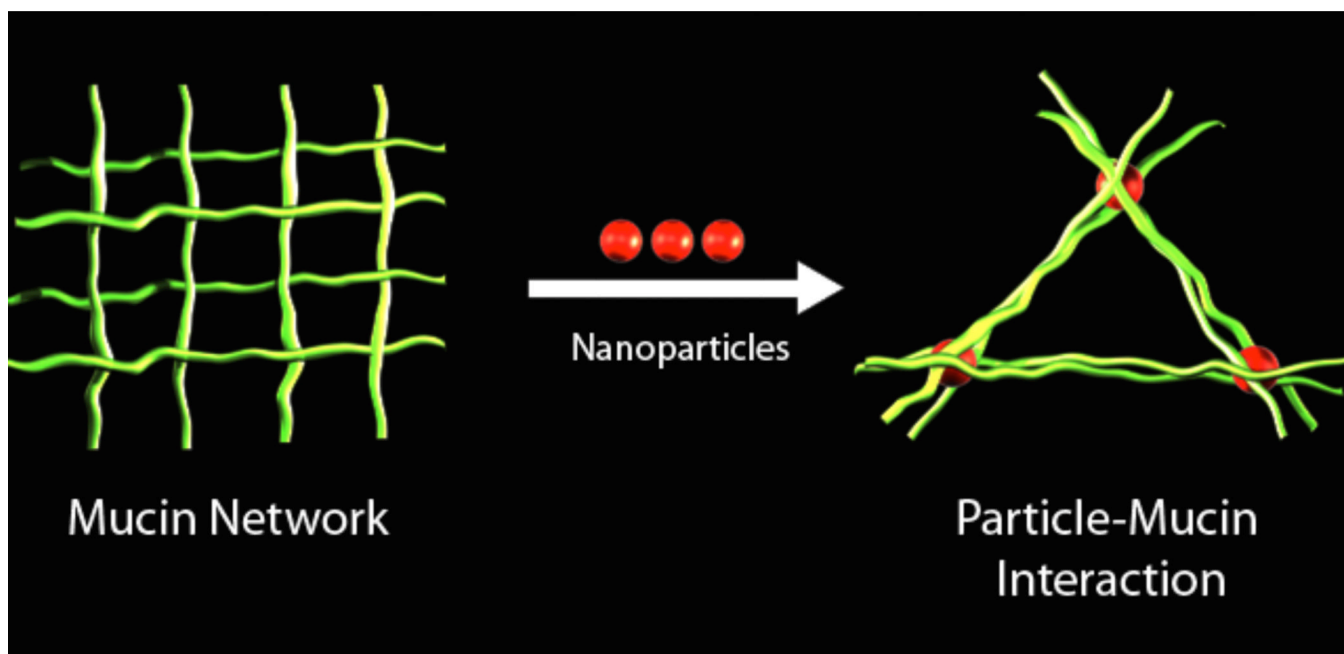


Figure 1. A scheme of particle induced disruption of mucus. A mucus fiber network is depicted at left with the introduction of particles (center) leading to an entanglement of particles with mucus resulting in a change of the fiber network.

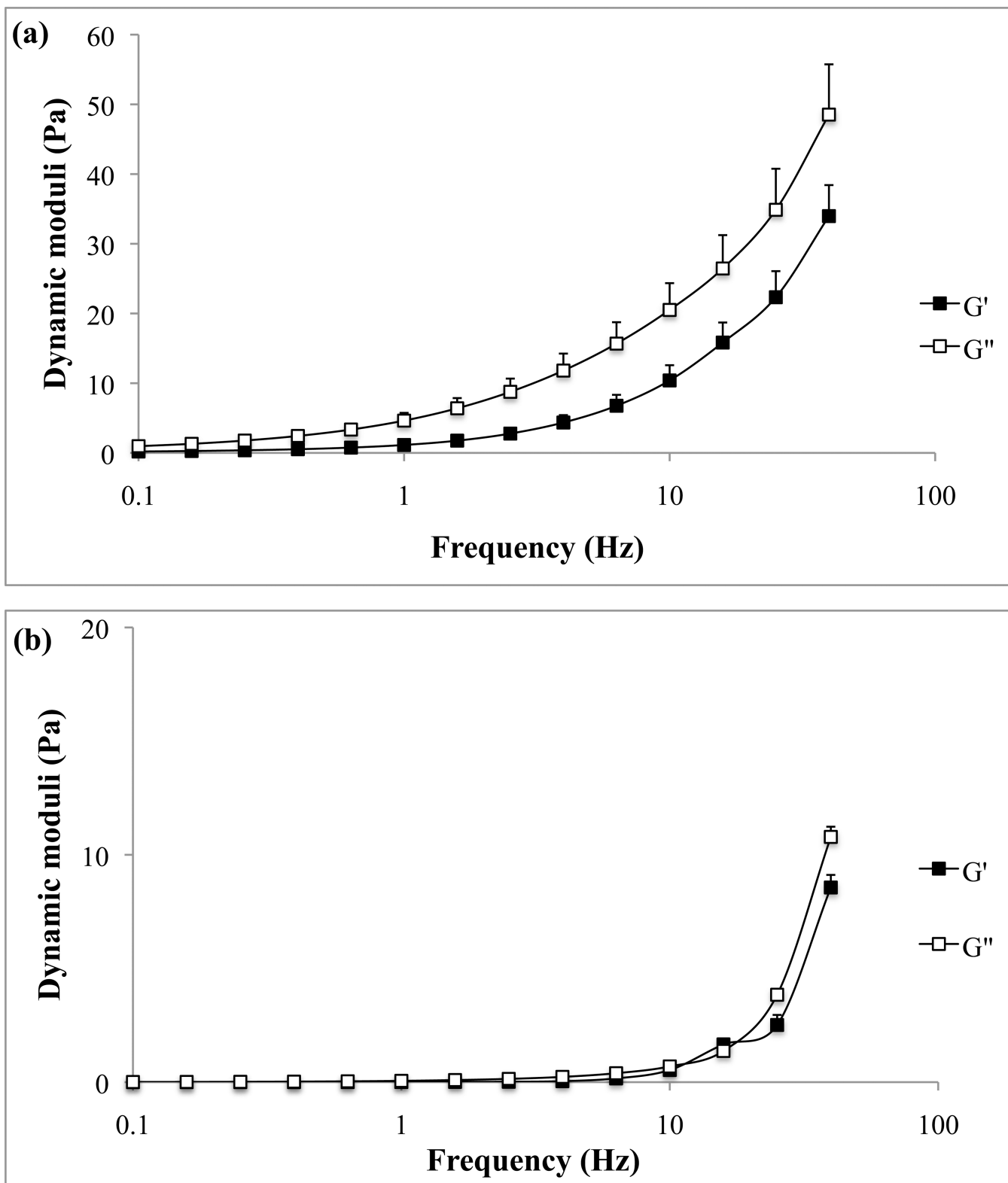
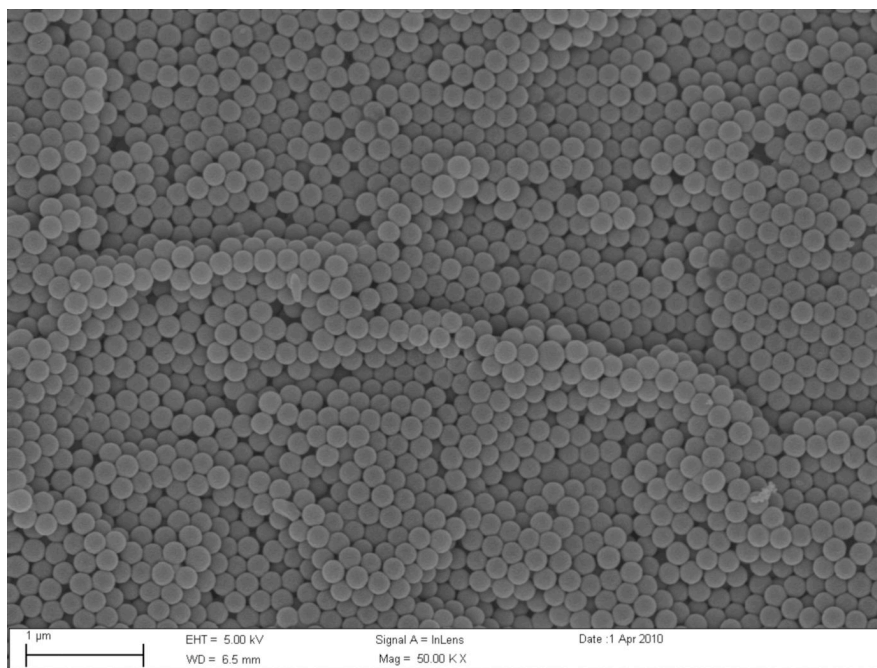


Figure 2.

Frequency sweep of the mucus model (a) and cystic fibrosis model (b). G' and G'' are plotted against frequency.



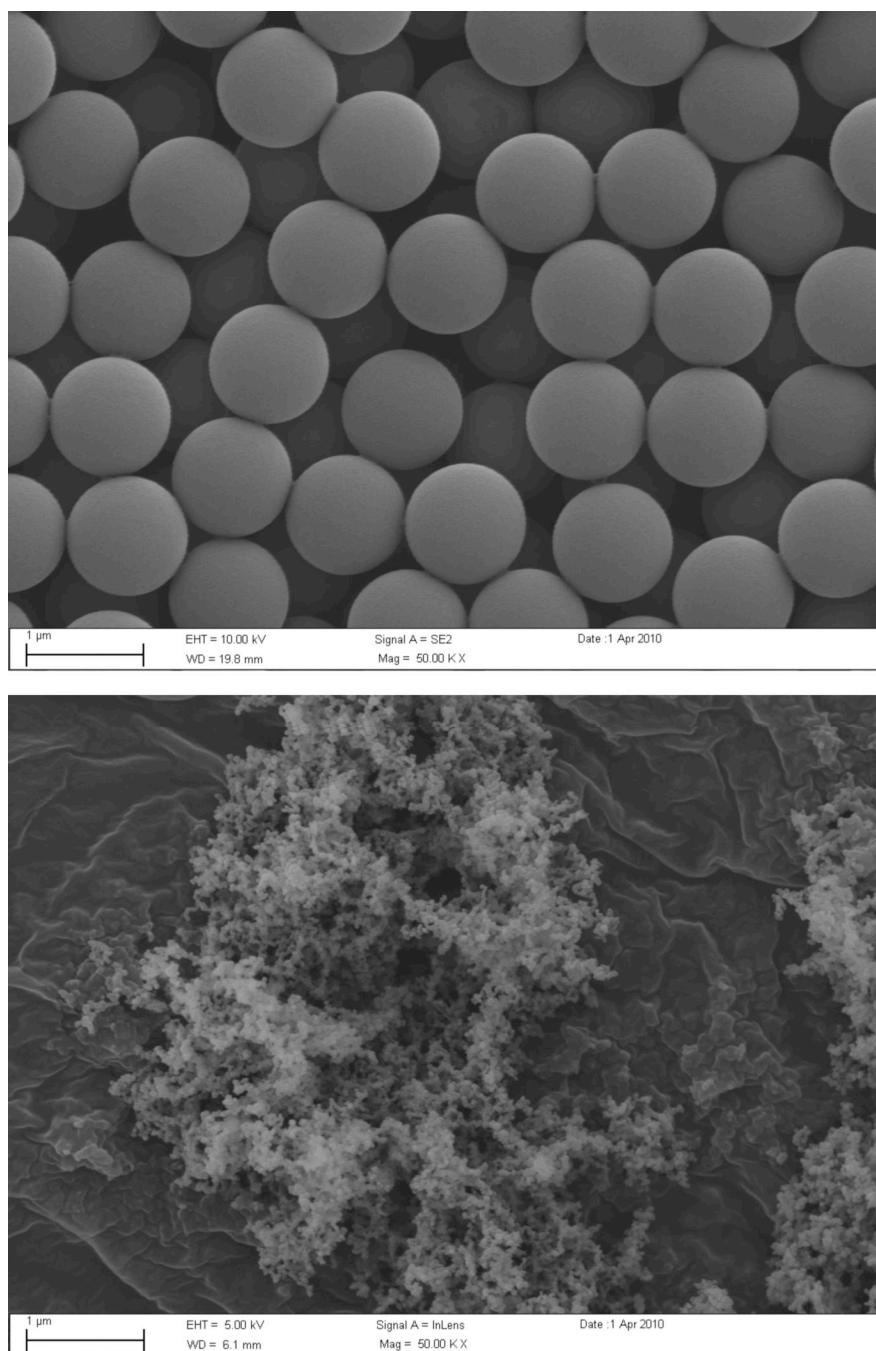


Figure 3. SEM images of carboxyl-modified 200 nm (a) and 1 micron (b) particles, and diesel particulate matter (c) were obtained at 50,000 × magnifications.

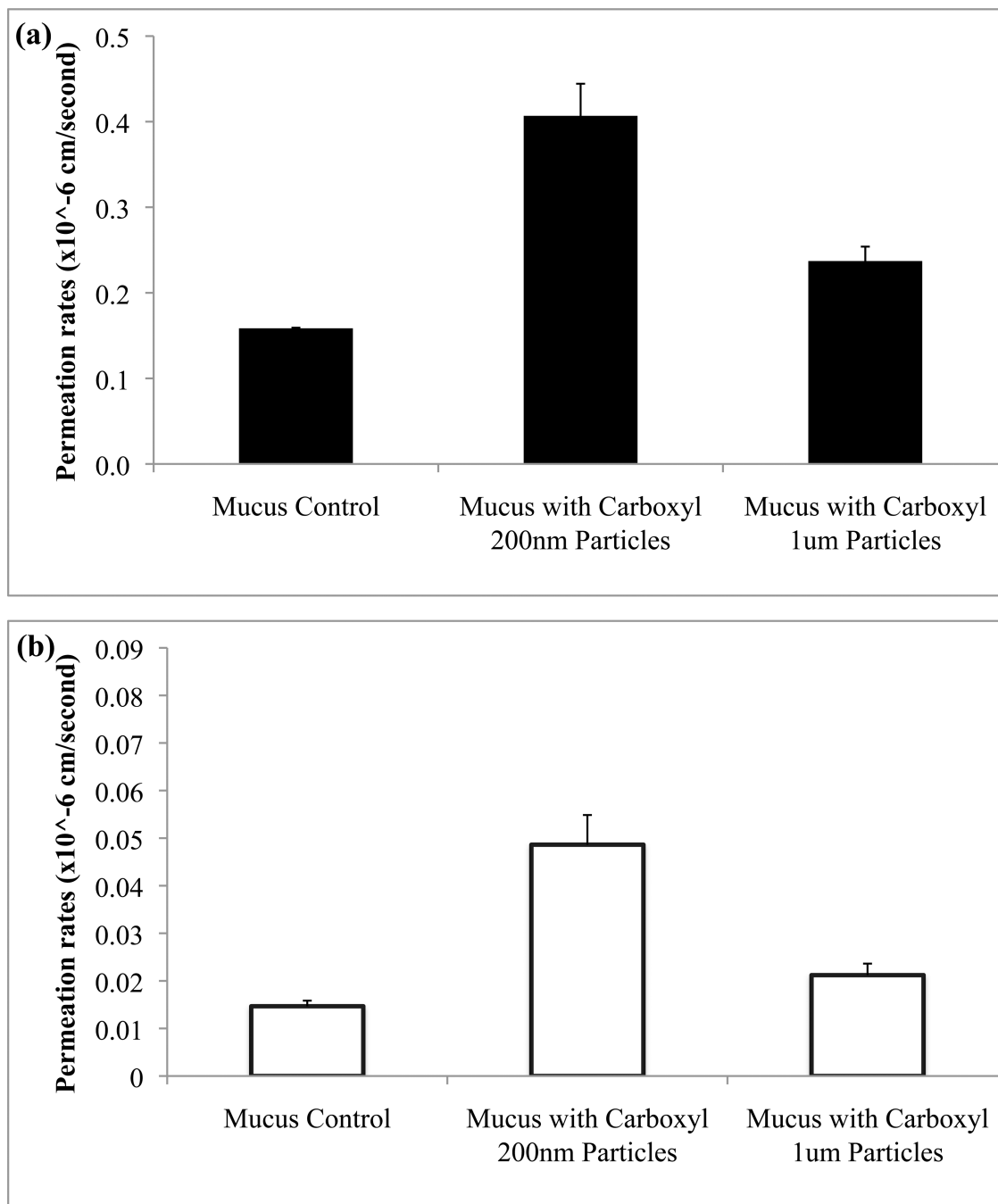


Figure 4.

The effect of carboxylated particle size (200 nm versus 1 micron) on permeation rates across a mucus model determined for fluorescein (a) and rhodamine B (b). For both drugs statistically significant ($p < 0.05$) differences were found for the 200 nm particles when compared to permeation rates of controls and 1 micron particles.

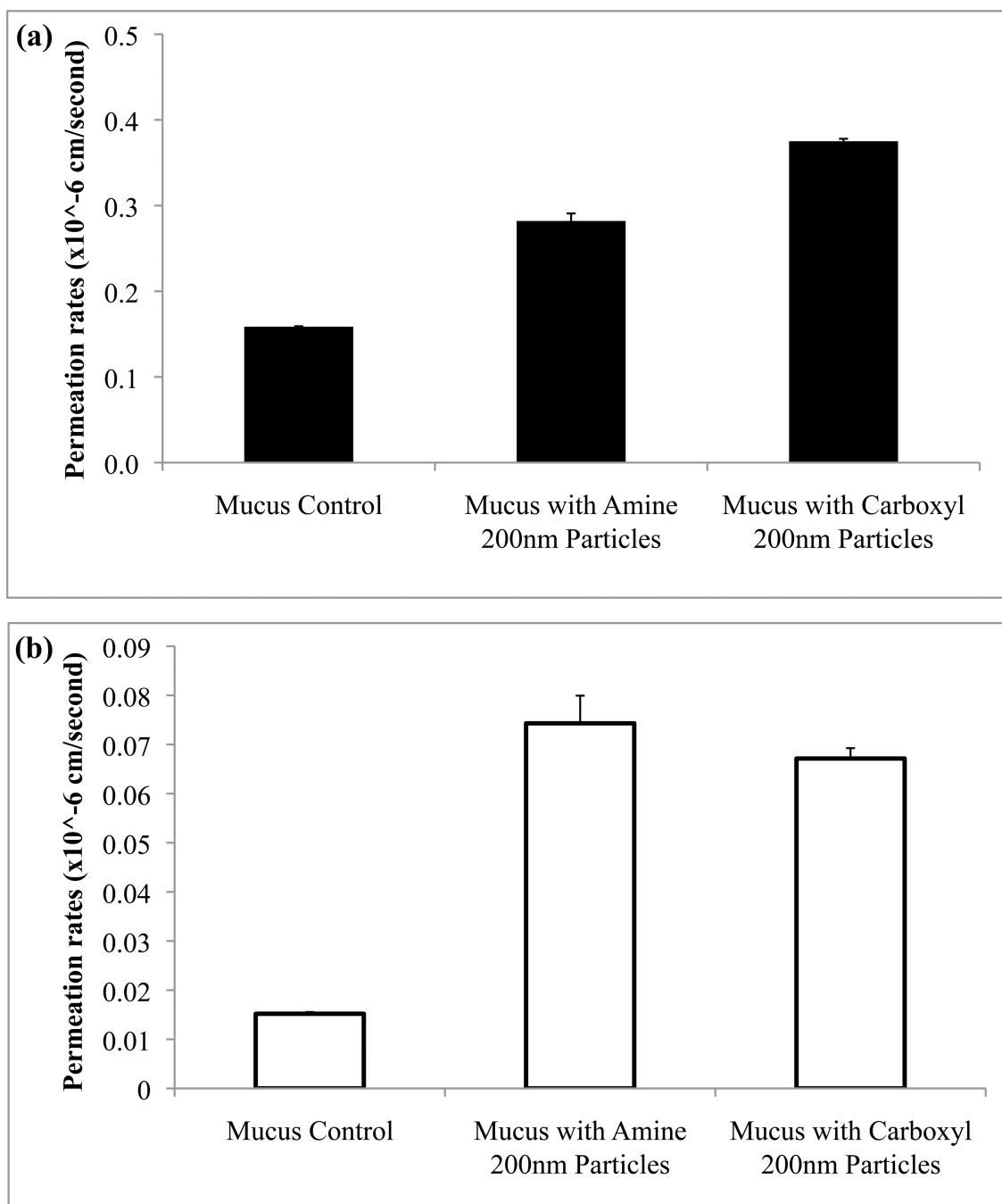


Figure 5. Permeation rates of fluorescein (a) and rhodamine B (b) were determined for mucus model that was treated with 200 nm particles with either amine or carboxyl functional groups when compared to control (no treatment). Statistical significance ($p < 0.05$) was seen for fluorescein with carboxylated particles.

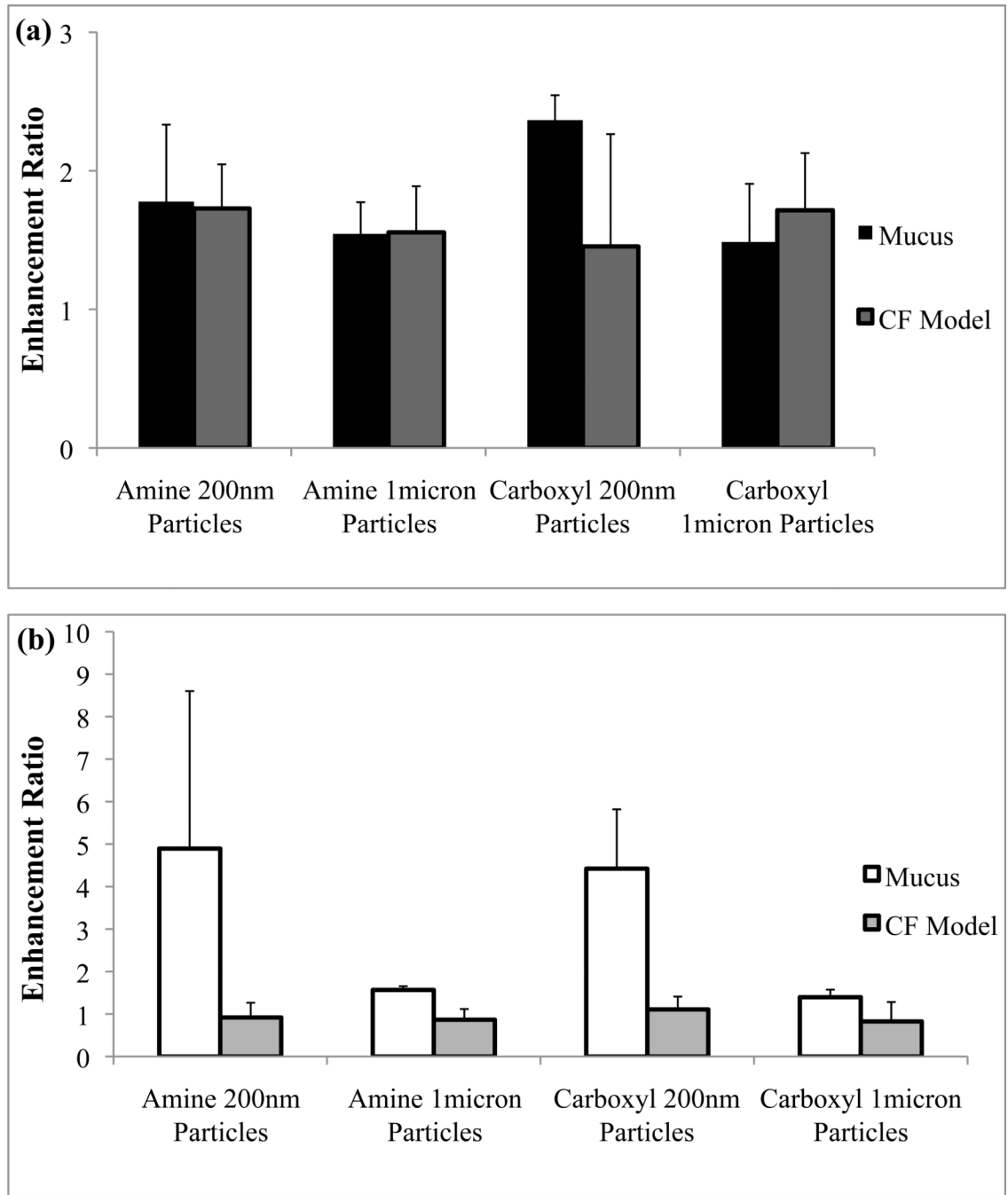


Figure 6. Enhancement ratios of either fluorescein (a) or rhodamine B (b) that were used in two different mucus models (mucus versus cystic fibrosis) were compared.

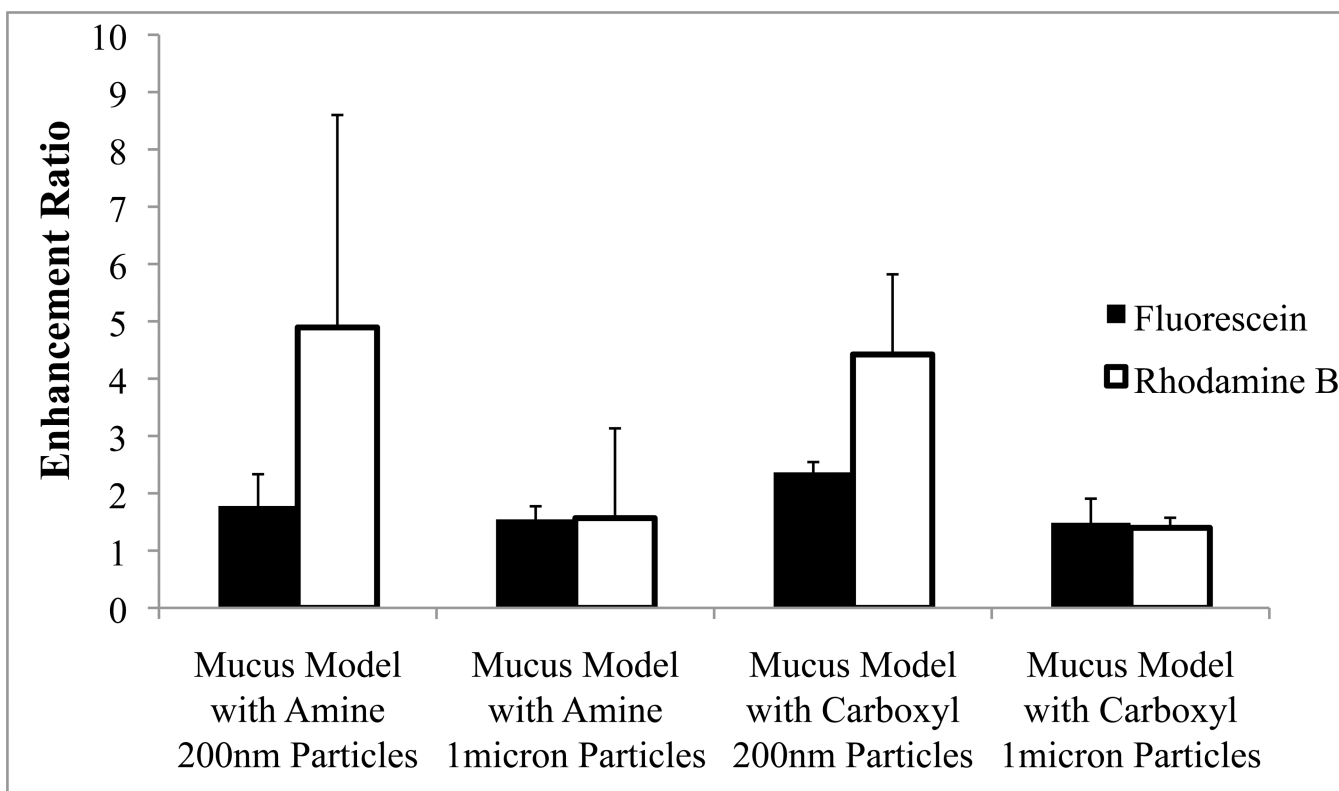


Figure 7. Fluorescein enhancement ratios were compared to that of rhodamine B within the mucus model.

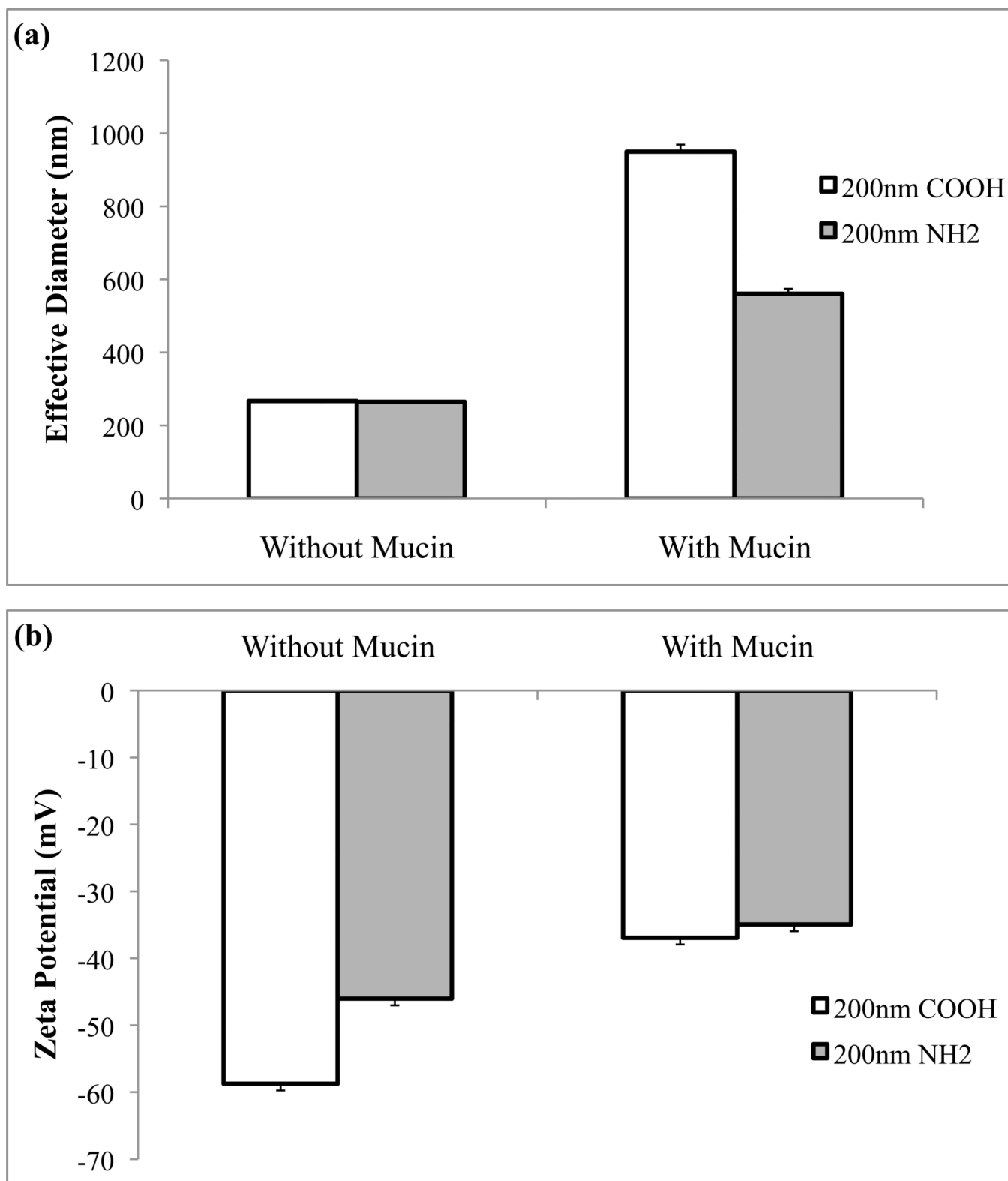
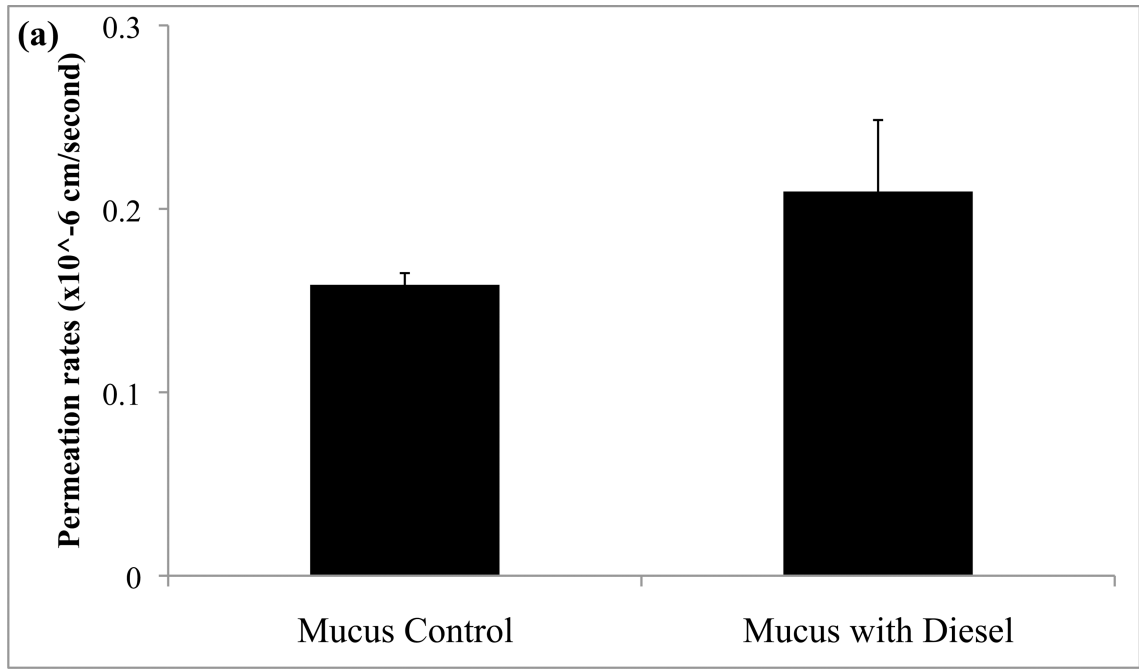


Figure 8.

Effective diameters were determined by dynamic light scattering (DLS; a) for 200 nm carboxyl and amine functionalized particles before and after mucus treatment. Zeta potentials (b) were then determined using the same conditions as the DLS measurements.



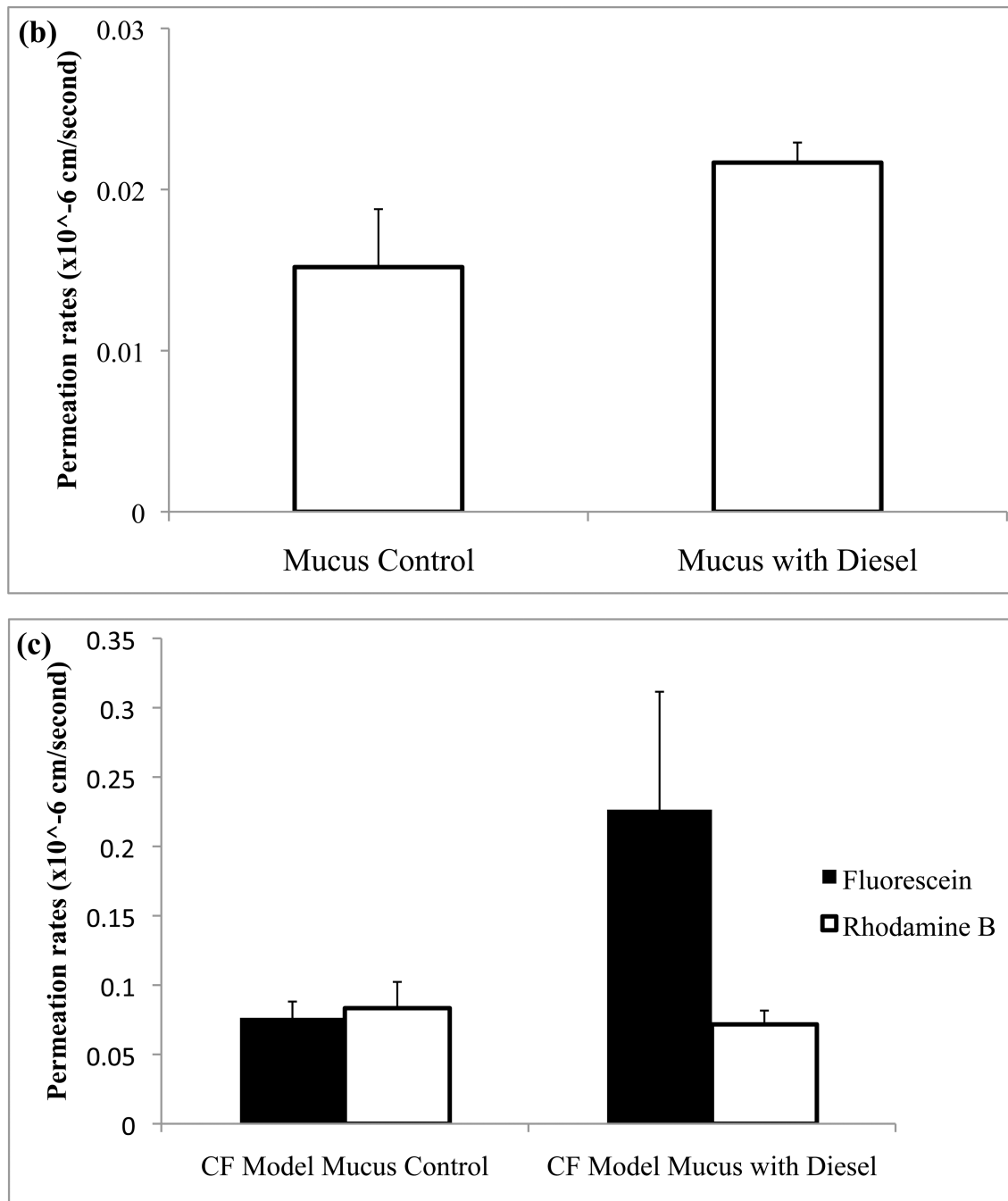


Figure 9.

Fluorescein (a) and rhodamine B (b) permeability were found before and after treatment of the mucus model with diesel particulate matter. Statistical significances ($p < 0.05$) were found for both fluorescein and rhodamine B with diesel treatment. Additionally, fluorescein ($p < 0.05$) and rhodamine B permeation rates were determined in the cystic fibrosis mucus model (c).